Published in final edited form as:
Bioorg Med Chem Lett. 2011 November 1; 21(21): 6533–6537. doi:10.1016/j.bmcl.2011.08.052.

Chemical scaffolds with structural similarities to siderophores of nonribosomal peptide-polyketide origin as novel antimicrobials against *Mycobacterium tuberculosis* and *Yersinia pestis*

Julian A. Ferreras[a,†], **Akash Gupta**[b,‡], **Neal D. Amin**[a,¥], **Arijit Basu**[c], **Barij N. Sinha**[c], **Stefan Worgall**[d], **Venkatesan Jayapraksh**[c,*], and **Luis E. N. Quadri**[b,*]

[a]Department of Microbiology and Immunology, Weill Medical College of Cornell University, New York, NY 10021, USA.

[b]Department of Biology, Brooklyn College, City University of New York, 2900 Bedford Avenue, Brooklyn, NY 11210, USA.

[c]Department of Pharmaceutical Sciences, Birla Institute of Technology, Mesra, Ranchi 835215, India.

[d]Department of Pediatrics and Genetic Medicine, Weill Medical College of Cornell University, New York, NY 10021, USA.

Abstract

Mycobacterium tuberculosis (Mtb) and *Yersinia pestis* (Yp) produce siderophores with scaffolds of nonribosomal peptide-polyketide origin. Compounds with structural similarities to these siderophores were synthesized and evaluated as antimicrobials against Mtb and Yp under iron-limiting conditions mimicking the iron scarcity these pathogens encounter in the host and under standard iron-rich conditions. Several new antimicrobials were identified, including some with increased potency in the iron-limiting condition. Our study illustrates the possibility of screening compound libraries in both iron-rich and iron-limiting conditions to identify antimicrobials that may selectively target iron scarcity-adapted bacteria and highlights the usefulness of building combinatorial libraries of compounds having scaffolds with structural similarities to siderophores to feed into antimicrobial screening programs.

Keywords

nonribosomal peptide; polyketide; siderophore; *Mycobacterium tuberculosis*; *Yersinia pestis*; antimicrobial compound; pyrazoline; hydroxyhydrazine

Mycobacterium tuberculosis (Mtb), the causative agent of tuberculosis, and *Yersinia pestis* (Yp), the etiologic agent of plague, are bacterial pathogens with serious impacts on global

*Corresponding authors: LENQ: Tel.: +1 (718) 951 5000 Ext. 6254, LQuadri@brooklyn.cuny.edu; JV: Tel.: +91-651-2275843, venkatesanj@bitmesra.ac.in .
†Current address: Department of Genetics, Universidad Nacional de Misiones, Posadas (3300), Misiones, Argentina.
‡Current address: Yale University School of Medicine, New Haven, CT 06510, USA.
¥Current address: University of California San Diego, School of Medicine, La Jolla, CA 92093, USA.

Supplementary Data Supplementary data associated with this article can be found, in the online version, at doi:

public health. Multidrug-resistant (MDR) tuberculosis is an emerging pandemic, whereas the more recent emergence of extensively drug-resistant (XDR) tuberculosis poses a new global threat.[1] Plague is a re-emerging disease for which the documented occurrence of MDR Yp strains and self-transferable Yp plasmids conferring antibiotic resistance raises concerns about future Plague control.[2] These grim scenarios underscore the need for expanding the anti-tuberculosis and anti-plague drug armamentarium.

Many bacteria utilize secreted, small (<1,000 Da) Fe^{3+}-chelating compounds (K_d $<10^{-25}$ M) called siderophores to scavenge Fe^{3+} from their microenvironments and transport it into the cell.[3] The Mtb siderophore (mycobactin/carboxymycobactin) and the Yp siderophore (yersiniabactin) are based on substituted scaffolds of nonribosomal peptide-polyketide origin (Figure 1).[4] Studies in cellular and animal models of infection have established the relevance of the mycobactin/carboxymycobactin and yersiniabactin siderophore systems in these pathogens.[5] The siderophores are believed to facilitate iron scavenging inside the host, where free iron is scarce (10^{-25}-10^{-15} M) and the pathogens experience and must adapt to iron-limiting conditions.[6] These observations suggest that the Mtb and Yp siderophore systems represent potential *in vivo* conditionally essential target candidates for the development of alternative therapeutics against tuberculosis and plague.[7]

We hypothesize that screening compounds with structural features resembling Mtb and Yp siderophores for growth inhibitory activity against these pathogens may lead to the discovery of novel antimicrobial scaffolds. Such novel antimicrobials could illuminate alternative paths to drug development and/or be useful as small-molecule tools to assist in the elucidation of new target candidates for drug development. Compounds with structural features resembling Mtb and Yp siderophores may impair the siderophore systems (*e.g.*, by inhibiting siderophore biosynthesis or transport) and halt bacterial growth in the host's iron-limiting environments. Alternatively, these compounds might gain access to the intracellular environment using siderophore transport systems and inhibit essential functions unrelated to iron acquisition. Consistent with these views, we have recently demonstrated potent antimicrobial activity against Mtb and Yp for novel diaryl-carbothioamide-pyrazoline derivatives with structural features resembling the hydroxyphenyl-oxazoline/thiazoline-containing half of Mtb and Yp siderophores.[8]

In an effort to identify additional novel inhibitors of Mtb and Yp growth, we synthesized and evaluated the antimicrobial activity of new 3,5-diaryl-substituted pyrazoline (DAP) derivatives (cmpds **1**–**22**,[9a] Table 1). In addition, we synthesized and tested the activity of a group of (2*E*)-2-benzylidene-*N*-hydroxyhydrazine carbo(ox/thio/oximid)-amide (BHHC) derivatives (cmpds **23**–**32**,[9b] Table 2) with hydroxyphenyl-cap functionalities resembling that of the siderophores. The compounds were tested for growth inhibitory activity against Mtb and Yp in iron-limiting media, which mimic the iron-scarcity condition that the pathogens encounter in the host, and in standard iron-rich media.[10a] We also assessed selected compounds for mode of action (bactericidal or bacteriostatic) in iron-limiting media and for cytotoxicity toward mammalian cells.[10b]

Testing against Mtb revealed that 17 compounds (**1**, **2**, **5**, **8**–**15**, **24**, **27**–**31**) had IC_{50}s and MICs (3–222 μM range, Table 3) within the concentration series tested in the iron-limiting medium, GASTD. Of these 17 compounds, 15 (**1**, **2**, **5**, **9**-**12**, **14**, **15**, **24**, **27**–**31**) also had determinable IC_{50}s and MICs (2–132 μM range) in the iron-rich medium, GASTD+Fe. Examination of $IC_{50GASTD+Fe}/IC_{50GASTD}$ and $MIC_{GASTD+Fe}/MIC_{GASTD}$ ratios revealed that the inhibitors had no noteworthy increased potency in the iron-limiting medium within the concentration series tested. This suggests that interference with iron acquisition, or any other bacterial process differentially required for growth under the iron-limiting condition, is not a property that significantly contributes to the compounds' antimicrobial activity against

Mtb. Interestingly, **14** is 5-fold more potent against Mtb cultured in GASTD+Fe, as judged by MIC values. This phenomenon might suggest that the mechanism(s) of action of **14** against Mtb might be potentiated by an elevated production of cytotoxic hydroxyl radicals originated through increased levels of Fenton reaction in the iron-rich medium. Such a potentiation would be in line with recent findings of Collins and coworkers regarding antibiotic-induced cell death.[16] Alternatively, **14** might inhibit an oxidative stress protection function(s) more critically needed in the iron-rich medium. Testing for cytotoxicity at the MIC against Mtb (125 μM) revealed that **14** had no significant cytotoxicity at short cell-cmpd contact time (4 hr), yet cell viability was reduced by 70% relative to untreated controls after prolonged contact time (24 hr) (Supplementary Data, Fig. S1).

Among the active DAP derivatives, **10** and **15** were the most potent against Mtb (IC_{50} = 7–4 μM, MIC = 16 μM, Table 3). Of these two cmpds, only **10** displayed significant cytotoxicity at the MIC against Mtb (16 μM). Cmpd **10** had a modest impact on cell viability, which was reduced only by 24% after 24 hr of cell-cmpd contact (Supplementary Data, Fig. S1). Encouragingly, these and most other inhibitors in the DAP derivatives series examined for mode of action against Mtb were bactericidal (>99% killing relative to inoculum) at concentrations of 1-2 × MIC_{GASTD} (Table 1). This finding is significant since bactericidal activity is a desirable property in any early lead compound evaluated for antibacterial drug development programs. It is worth noting that the only two compounds (**11** and **12**) defined as bacteriostatic in Table 1 showed significant bactericidal activity, yet below the 99% killing criterion set in this study for defining bactericidal mode of action. Among the compounds of the BHHC derivatives series with defined IC_{50} and MIC values, **27** and **29** were the most active against Mtb (IC_{50} = 2–4 μM, MIC = 6–10 μM, Table 3). These two compounds displayed no significant cytotoxicity in mammalian cells at their respective MIC values determined against Mtb (Supplementary Data, Fig. S1). Gratifyingly, **27**, **29** and other active cmpds in this series displayed bactericidal mode of action against Mtb at concentrations of 1.7-4 × MIC_{GASTD} (Table 3).

Testing against Yp revealed that 14 cmpds (**1**, **2**, **7**–**9, 11**, **13**, **14**, **19**, **27**–**29**, **31**, **32**; Table 1) reached IC_{50}s (0.04–181 μM range, Table 4) within the concentration series tested in the iron-limiting medium, PMHD. Nine of these compounds (**1**, **11, 13**, **14**, **27**–**29**, **31**, **32**) also reached MICs (0.2–388 μM range) in PMHD. Only **29** and **30** had determinable activity in the iron-rich medium, PMHD+Fe (**29**: IC50 = 156 μM, MIC = 233 μM; **30**: IC50 = 305 μM). Interestingly, examination of the $IC_{50PMHD+Fe}/IC_{50PMHD}$ ratios revealed that a number of inhibitors (**7**, **11**, **13**, **14**, **19**, **27**, **29**, **31**, **32**) with increased potency (>3-fold) against Yp cultured under iron scarcity. Cmpd **32**, with >100-fold and >20-fold higher potency in PMHD based on IC_{50} and MIC values, respectively, stood out in this group. The higher potency of these compounds in the iron-limiting medium raises the possibility that interference with an iron acquisition function, or other function more critically required for growth under the iron-limiting condition, is a property that significantly contributes to the compounds' antimicrobial activity against Yp. One of the possible mechanisms of action of these compounds could be related to iron-binding properties. An iron-binding ability strong enough to outcompete the powerful iron chelating capacity of the bacterial siderophore could lead to sequestration of the traces of iron in the iron-limiting medium, thus reducing further iron bioavailability and producing a stronger antimicrobial activity under the iron-scarcity condition. Alternatively, it is possible that these compounds gain intracellular access using the iron-scarcity-unregulated yersiniabactin's uptake system,[5e] therefore reducing IC_{50} and MIC values in PMHD.

Compounds **13** (IC_{50PMHD} = 4 μM, MIC_{PMHD} = 16 μM) and **14** (IC_{50PMHD} = 5 μM, MIC_{PMHD} = 21 μM) were the most potent among the active DAP derivatives with detectable activity against Yp (Table 4). These two compounds displayed no significant cytotoxicity

when they were evaluated at their respective MIC values determined against Yp (Supplementary Data, Fig. S1). Testing of these and two other active DAP derivatives (**1**, **11**) for mode of action against Yp revealed that the four compounds were bacteriostatic at concentrations of 1-2 × MIC_{PMHD} (Table 4). Among the BHHC derivatives with defined IC_{50} and MIC values in at least one condition (iron limiting or iron rich), **32** stood out due to its remarkable potency (IC_{50PMHD} = 0.04 μM, MIC_{PMHD} = 0.2 μM) against Yp cultured under iron scarcity. Encouragingly, **32** displayed no significant cytotoxicity when evaluated in cytotoxicity assays at the MIC determined against Yp (Supplementary Data, Fig. S1). Notably, the activity of **32** was significantly higher than that of streptomycin (IC_{50} and MIC ~1 μM), a bactericidal drug used to treat plague and included herein as an anti-Yp activity reference. Five compounds (**27**-**29**, **31**, **32**) of the BHHC derivatives series were tested for mode of action against Yp in PMHD at concentrations of 1-2 × MIC_{PMHD}. Under the conditions tested, **29** displayed bactericidal activity, whereas **27**, **28**, **31** and **32** were bacteriostatic.

In sum, 20 of 32 compounds synthesized and evaluated herein have detectable antimicrobial against Mtb and/or Yp in at least one condition, iron scarcity or iron sufficient. To our knowledge, these are novel scaffolds not previously shown to have antimicrobial properties. Most active compounds identified herein have comparable potency in the low and high iron conditions. This finding suggests that their pharmacological targets are likely to be essential bacterial functions required under both these conditions. In line with our aforementioned hypothesis, however, some of our compounds have higher potency under the iron-limiting condition. Under this condition, bacteria depend on siderophores for efficient iron scavenging and engage an adaptive response to tailor their physiology to iron scarcity, thus exposing novel potential *in vivo* conditional target candidates.[7a] Some of these antimicrobials may impair siderophore system functioning as discussed above, a property that would result in bacteriostatic activity conditional to environmental iron scarcity (*e.g.*, as seen with **27** and **32** against Yp). Overall, our study illustrates the possibility of screening compound libraries in both iron-sufficient and iron-limiting conditions to identify antimicrobials that may selectively target iron scarcity-adapted bacteria and highlights the usefulness of building combinatorial libraries of compounds having scaffolds with structural similarities to siderophores to feed antimicrobial screening programs.

Supplementary Material

Refer to Web version on PubMed Central for supplementary material.

Acknowledgments

This work was supported by NIH Grant 1R01AI075092-01A1 (LENQ). LENQ acknowledges the endowment support from Carol and Larry Zicklin. We are grateful to the Sophisticated Analytical Instrument Facility (CDRI, Lucknow, India) for providing spectral data.

References and Notes

1 (a). Dye C. Global epidemiology of tuberculosis. Lancet. 2006; 367:938. [PubMed: 16546542] (b) Gandhi NR, Moll A, Sturm AW, Pawinski R, Govender T, Lalloo U, Zeller K, Andrews J, Friedland G. Extensively drug-resistant tuberculosis as a cause of death in patients co-infected with tuberculosis and HIV in a rural area of South Africa. Lancet. 2006; 368:1575. [PubMed: 17084757] (c) Zignol M, Hosseini MS, Wright A, Weezenbeek CL, Nunn P, Watt CJ, Williams BG, Dye C. Global incidence of multidrug-resistant tuberculosis. J. Infect. Dis. 2006; 194:479. [PubMed: 16845631]

2 (a). Galimand M, Guiyoule A, Gerbaud G, Rasoamanana B, Chanteau S, Carniel E, Courvalin P. Multidrug resistance in *Yersinia pestis* mediated by a transferable plasmid. N. Engl. J. Med.

1997; 337:677. [PubMed: 9278464] (b) Guiyoule A, Gerbaud G, Buchrieser C, Galimand M, Rahalison L, Chanteau S, Courvalin P, Carniel E. Transferable plasmid-mediated resistance to streptomycin in a clinical isolate of *Yersinia pestis*. Emerg. Infect. Dis. 2001; 7:43. [PubMed: 11266293]

3 (a). Ratledge C, Dover LG. Iron metabolism in pathogenic bacteria. Annu. Rev. Microbiol. 2000; 54:881. [PubMed: 11018148] (b) Drechsel, H.; Winkelmann, G. Iron chelation and siderophores. In: Winkelmann, G.; Carrano, CJ., editors. Transition metals in microbial metabolism. Harwood Accademic; Amsterdam: 1997. p. 1(c) Neilands JB. Siderophores: structure and function of microbial iron transport compounds. J. Biol. Chem. 1995; 270:26723. [PubMed: 7592901] (d) Wooldridge KG, Williams PH. Iron uptake mechanisms of pathogenic bacteria. FEMS Microbiol. Rev. 1993; 12:325. [PubMed: 8268005] (e) Wandersman C, Delepelaire P. Bacterial iron sources: from siderophores to hemophores. Annu. Rev. Microbiol. 2004; 58:611. [PubMed: 15487950]

4. Quadri LEN. Assembly of aryl-capped siderophores by modular peptide synthetases and polyketide synthases. Mol. Microbiol. 2000; 37:1. [PubMed: 10931301]

5 (a). De Voss JJ, Rutter K, Schroeder BG, Su H, Zhu Y, Barry CE III. The salicylate-derived mycobactin siderophores of *Mycobacterium tuberculosis* are essential for growth in macrophages. Proc. Natl. Acad. Sci. USA. 2000; 97:1252. [PubMed: 10655517] (b) Rodriguez GM, Smith I. Identification of an ABC transporter required for iron acquisition and virulence in *Mycobacterium tuberculosis*. J. Bacteriol. 2006; 188:424. [PubMed: 16385031] (c) Bearden SW, Fetherston JD, Perry RD. Genetic organization of the yersiniabactin biosynthetic region and construction of avirulent mutants in *Yersinia pestis*. Infect. Immun. 1997; 65:1659. [PubMed: 9125544] (d) Fetherston JD, Bertolino VJ, Perry RD. YbtP and YbtQ: two ABC transporters required for iron uptake in *Yersinia pestis*. Mol. Microbiol. 1999; 32:289. [PubMed: 10231486] (e) Fetherston JD, Kirillina O, Bobrov AG, Paulley JT, Perry RD. The yersiniabactin transport system is critical for the pathogenesis of bubonic and pneumonic plague. Infect. Immun. 2010; 78:2045. [PubMed: 20160020]

6 (a). Jurado RL. Iron, infections, and anemia of inflammation. Clin. Infect. Dis. 1997; 25:888. [PubMed: 9356804] (b) Ward CG, Bullen JJ, Rogers HJ. Iron and infection: new developments and their implications. J. Trauma. 1996; 41:356. [PubMed: 8760553]

7 (a). Quadri LEN. Strategic paradigm shifts in the antimicrobial drug discovery process of the 21st century. Infect. Disord. Drug Targets. 2007; 7:230. [PubMed: 17897059] (b) Ferreras JA, Ryu JS, Di Lello F, Tan DS, Quadri LE. Small-molecule inhibition of siderophore biosynthesis in *Mycobacterium tuberculosis* and *Yersinia pestis*. Nat. Chem. Biol. 2005; 1:29. [PubMed: 16407990]

8. Stirrett KL, Ferreras JA, Jayaprakash V, Sinha BN, Ren T, Quadri LE. Small molecules with structural similarities to siderophores as novel antimicrobials against *Mycobacterium tuberculosis* and *Yersinia pestis*. Bioorg. Med. Chem. Lett. 2008; 18:2662. [PubMed: 18394884]

9 (a). Cmpds **1**–**14** were synthesized from appropriate 2′-hydroxy chalcone derivatives as outlined in Scheme 1 (Supplementary Data). Cmpds **9** and **10** were prepared as we reported earlier.[11] 1*N*-acetyl pyrazolines (**3** and **4**) were obtained by refluxing appropriate 2′-hydroxy chalcones with hydrazine hydrate (80%) in acetic acid.[12] Similarly, **5** and **6** as well as **11** and **12** were obtained by refluxing appropriate 2′-hydroxy chalcones with semicarbazide hydrochloride/ aminoguanidine bicarbonate in methanol for 4–6 hr. Cmpds **7** and **8** were synthesized from **1** and **2**, respectively. Ethyl chloroformate was added to a solution of pyrazolines (**1** and **2**) in methanol with constant stirring at room temperature. Triethylamine was added to neutralize the acid liberated. Hydroxylamine in methanol was then added with stirring at room temperature for 2 hr to obtain **7** and **8**. Cmpds **13** and **14** were synthesized from **9** and **9a**, respectively. A slight excess of methyl iodide was added to **9** and **9a** dropwise with stirring (<10°C, 1h). Hydroxylamine in methanol was then added and stirring continued (22°C, 30 min) to obtain **13** and **14**. Cmpds **15**–**22** were synthesized from appropriate 2′-hydroxy chalcone derivatives as outlined in Scheme 2 (Supplementary Data). Cmpds **15** and **16** were prepared in similar manner to **5** and **6** and by replacing semicarbazide hydrochloride with isoniazide. Cmpds **17**–**22** were prepared from **1** and **2** as we reported earlier.[13] Reaction of benzoyl chloride with **1** and **2** in pyridine provided **17** and **18**, respectively. Similarly, reaction of sulphonyl chlorides with **1** and **2** in THF provided **19**–**22**. Cmpds **23**–**32** were synthesized as outlined in Scheme 3 (Supplementary

Data). (b) Cmpds **23**–**26** were prepared as reported.[14] *N*-hydroxy semicarbazides were prepared by reaction of hydroxylamine, phenylchloroformate and hydrazine hydrate (80%) in moist ether. The *N*-hydroxy semicarbazides were then condensed with appropriate aldehyde/ketone to yield **23**–**26**. Methyl hydrazinecarbodithioate was prepared as reported[15] and condensed with appropriate aldehyde/ketone to produce **27**–**29**. Cmpds **30** and **31** were prepared by a strategy similar to that used for **13** and **14**. A slight excess of methyl iodide followed by hydroxylamine to thiosemicarbazones of appropriate aldehydes provided **30** and **31**. Cmpds **32** was synthesized as we described earlier.[15a] Reaction of **27** with *N*-hydroxypiperidine-4-carboxamide provided **32**. The intermediates were characterized by elemental analysis and FT-IR spectra. Final cmpds were characterized through ^{1}H-NMR and FAB-MS spectral data. Synthetic procedures, physicochemical and spectral characteristics of **1**–**32** are presented in Supplementary Data.

10 (a). Antimicrobial activity was determined in dose–response experiments using 96-well-plate-based, twofold-microdilution assays as reported.[7b,8,17] Virulent *Mtb* H37Rv was grown in iron-limiting GASTD medium and GASTD supplemented with 100 μM $FeCl_3$ (GASTD+Fe).[7b,17] Avirulent *Yp* KIM6-2082.1+ was grown in iron-limiting PMHD medium and PMHD supplemented with 100 μM $FeCl_3$ (PMHD+Fe).[7b,17] Cultures were started (OD_{600} = 0.001) from deferrated culture stocks prepared as reported.[7b] Growth was assessed as OD_{600} after incubation at 37 °C (*Mtb*: 10 days, stationary condition; *Yp*: 26 hr, 200 rpm) using a Spectra Max Plus reader (Molecular Dynamics). Compounds were evaluated at up to the highest concentration permitted by their solubility, with a 500 μM upper testing limit, and added as DMSO solutions. DMSO was kept at 0.5% in treated and DMSO-control cultures. IC_{50}s were calculated from sigmoidal curves fitted to triplicate dose–response data using KaleidaGraph (Synergy Software) as reported.[7b] MIC_{90}s were calculated as the lowest concentration tested that inhibited growth by ≥90% relative to DMSO controls. Compounds were tested at up to the maximum multiple of the MIC permitted by their solubility. (b) After bacterial cultures were treated with compounds and incubated as noted above, the mode of action was evaluated by enumerating CFU/mL after plating serial 10-fold dilutions of duplicate *Mtb* and *Yp* cultures on plates of Middlebrook 7H11[18] and plates of TBA[17], respectively. Plates were incubated at 37 °C for 30 days for *Mtb* and at 30 °C for 3 days for *Yp* before colony counting. Cytotoxicity was assessed against HeLa cells in a 96-well plate platform using a standard ATPLite™ reagent-based cytotoxicity assay (Perkin-Elmer) as previously reported.[8]

11 (a). Azarifar D, Shaabanzadeh M. Synthesis and characterization of new 3,5-dinaphthyl substituted 2-pyrazolines and study of their antimicrobial activity. Molecules. 2002; 7:885.(b) Gökhan N, Yeşilada A, Uçar G, Erol K, Bilgin AA. 1-*N*-substituted thiocarbamoyl-3-phenyl-5-thienyl-2-pyrazolines: Synthesis and evaluation as MAO inhibitors. Arch. Pharm. Pharm. Med. Chem. 2003; 336:362.(c) Rao YK, Fang SH, Tzeng YM. Differential effects of synthesized 2′-oxygenated chalcone derivatives: modulation of human cell cycle phase distribution. Bioorg. Med. Chem. 2004; 12:2679. [PubMed: 15110849]

12. Tai AW, Lien EJ, Moore EC, Chun Y, Roberts JD. Studies of N-hydroxy-N'-aminoguanidine derivatives by nitrogen-15 nuclear magnetic resonance spectroscopy and as ribonucleotide reductase inhibitors. J. Med. Chem. 1983; 6:1326. [PubMed: 6350588]

13. Sharma TC, Saksena V, Reddy NJ. Oxidation of some hydroxy aryl pyrazolines with manganese dioxide. Acta Chim. Acad. Sci. Hungar. 1977; 93:415.

14. Klayman DL, Bartosevich JF, Griffin TS, Mason CJ, Scovill JP. 2-Acetylpyridine thiosemicarbazones. 1. A new class of potential antimalarial agents. J. Med. Chem. 1979; 22:855. [PubMed: 376848]

15 (a). Bhadaliya C, Bunha M, Jagrat M, Sinha BN, Saiko P, Graser G, Szekeres T, Raman G, Rajendran P, Moorthy D, Basu A, Venkatesan J. Design, synthesis and anticancer activity of piperazine hydroxamates and their histone deacetylase (HDAC) inhibitory activity. Bioorg. Med. Chem. Lett. 2010; 20:3906. [PubMed: 20605448] (b) Ren S, Wang R, Komatsu K, Bonaz-Krause P, Zyrianov Y, McKenna CE, Csipke C, Tokes ZA, Lien EJ. Synthesis, biological evaluation, and quantitative structure-activity relationship analysis of new Schiff bases of hydroxysemicarbazide as potential antitumor agents. J. Med. Chem. 2002; 45:410. [PubMed: 11784145]

16 (a). Dwyer DJ, Kohanski MA, Hayete B, Collins JJ. Gyrase inhibitors induce an oxidative damage cellular death pathway in *Escherichia coli*. Mol. Syst. Biol. 2007; 3:91. [PubMed: 17353933] (b)

Kohanski MA, Dwyer DJ, Collins JJ. How antibiotics kill bacteria: from targets to networks. Nat. Rev. Microbiol. 2010; 8:423. [PubMed: 20440275] (c) Kohanski MA, Dwyer DJ, Hayete B, Lawrence CA, Collins JJ. A common mechanism of cellular death induced by bactericidal antibiotics. Cell. 2007; 130:797. [PubMed: 17803904]

17. Stirrett KL, Ferreras JA, Rossi SM, Moy RL, Fonseca FV, Quadri LE. A multicopy suppressor screening approach as a means to identify antibiotic resistance determinant candidates in *Yersinia pestis*. BMC Microbiol. 2008; 8:122. [PubMed: 18644132]

18 (a). Chavadi SS, Edupuganti UR, Vergnolle O, Fatima I, Singh SM, Soll CE, Quadri LE. Inactivation of *tesA* reduces cell-wall lipid production and increases drug susceptibility in mycobacteria. J. Biol. Chem. 2011(b) Ferreras JA, Stirrett KL, Lu X, Ryu JS, Soll CE, Tan DS, Quadri LE. Mycobacterial phenolic glycolipid virulence factor biosynthesis: mechanism and small-molecule inhibition of polyketide chain initiation. Chem. Biol. 2008; 15:51. [PubMed: 18158259]

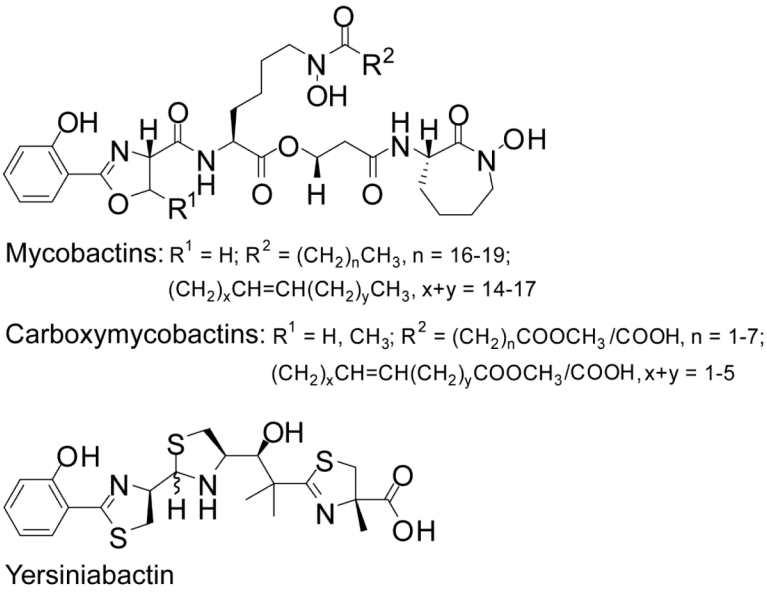

Figure 1.
Structures of *M. tuberculosis* and *Y. pestis* siderophores.

Table 1

3.5-Diarvl-substituted pyrazoline (DAP) derivatives (**1–22**)

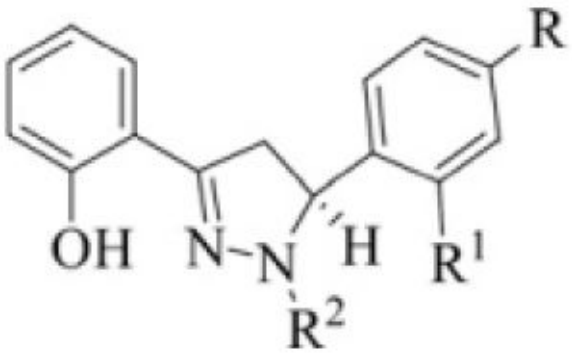

Compound	R	R’	R
1	–H	–OH	–H
2	–OH	–H	–H
3	–H	–OH	
4	–OH	–H	
5	–H	–OH	
6	–OH	–H	
7	–H	–OH	
8	–OH	–H	
9	–H	–OH	
10	–H	–CH_3	
11	–H	–OH	
12	–OH	–H	

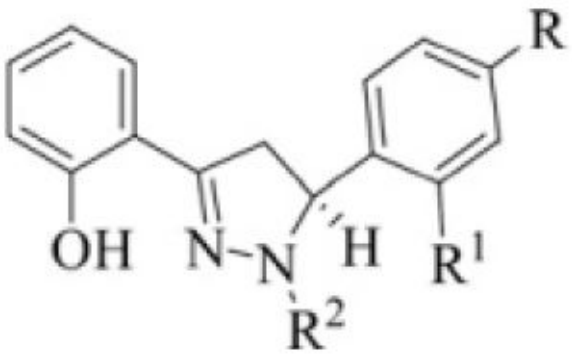

Compound	R	R’	R
13	–H	–OH	
14	–OH	–H	
15	–H	–OH	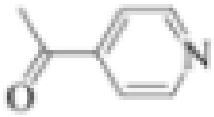
16	–OH	–H	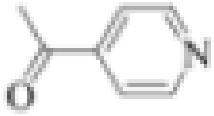
17	–H	–OH	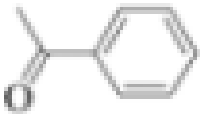
18	–OH	–H	
19	–H	–OH	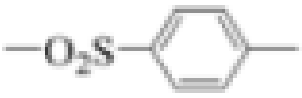
20	–OH	–H	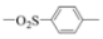
21	–H	–OH	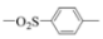
22	–OH	–H	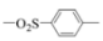

Table 2

(2*E*)-2-Benzylidene-*N*-hydroxyhydrazine carbo(ox/thio/oximid)-amide (BHHC) derivatives (**23–32**)

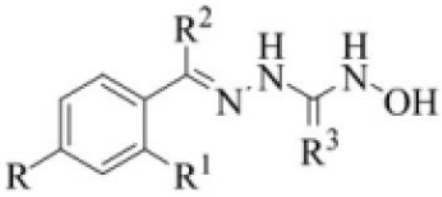

Cmpds **23-26, 30, 31**

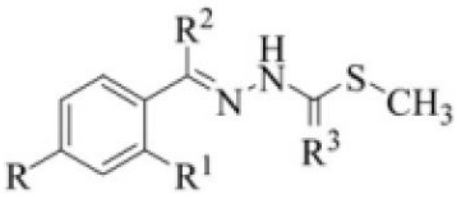

Cmpds **27-29**

Compound	R	R^1	R^2	R^3
23	–H	–OH	–H	=O
24	–OH	–H	–H	=O
25	–H	–OH	$-CH_3$	=O
26	–OH	–H	$-CH_3$	=O
27	–H	–OH	–H	=S
28	–OH	–H	–H	=S
29	–H	–OH	$-CH_3$	=S
30	–H	–OH	–H	–NH
31	–OH	–H	–H	–NH
32	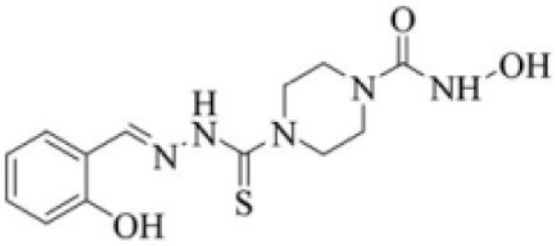			

Table 3

Antimicrobial activity against *M. tuberculosis*

Compound	IC_{50}[a] (μM)		Ratio	MIC_{90}[b] (μM)		Ratio	Mode of action[c]
	GASTD+Fe	GASTD		GASTD+Fe	GASTD		
DAP series							
1	18	25	1	59	66	1	BC (2 × MIC)
2	37	46	1	125	125	1	BC (I × MIC)
3	>16	>31	nd	>16	>32	nd	nd
4	>8	>8	nd	>8	>8	nd	nd
5	64	77	1	104	208	0.5	BC (2 × MIC)
6	>32	>63	nd	>63	>63	nd	nd
7	>32	54	nd	>31	>63	nd	nd
8	40	42	1	>31	125	nd	BC (1 × MIC)
9	50	53	1	125	125	1	BC (2 × MIC)
10	7	7	1	16	16	1	BC (2 × MIC)
11	23	44	1	66	66	1	BC (2 × MIC)[d]
12	26	31	1	76	125	1	BC (2 × MIC)[d]
13	32	37	1	>125	125	>l	BC (2 × MIC)
14	22	47	0.5	31	125	0.2	BC (2 × MIC)
15	8	8	1	16	16	1	BC (2 × MIC)
16	>4	>8	nd	>4	>8	nd	nd
17	98	84	1	>500	>500	nd	nd
18	>16	>63	nd	>63	>63	nd	nd
19	>16	>63	nd	>31	>63	nd	nd
20	>31	>63	nd	>31	>63	nd	nd
21	>31	>63	nd	>31	>63	nd	nd
22	>31	>63	nd	>31	>63	nd	nd
BHHC series							
23	>16	>16	nd	>16	>16	nd	nd
24	40	97	0.4	97	146	1	BC (2 × MIC)
25	>8	>8	nd	>8	>8	nd	nd

Compound	IC_{50}[a] (μM)		Ratio	MIC_{90}[b] (μM)		Ratio	Mode of action[c]
	GASTD+Fe	GASTD		GASTD+Fe	GASTD		
26	>500	>500	nd	>500	>500	nd	nd
27	2	3	1	6	7	1	BC (4 × MIC)
28	33	31	1	59	59	1	BC (2 × MIC)
29	4	4	1	9	10	1	BC (2 × MIC)
30	15	11	1	26	222	1	BC (2 × MIC)
31	43	43	1	132	222	1	BC (2 × MIC)
32	>8	20	nd	>8	>31	nd	nd
Isoniazid	0.09	0.07	1	0.2	0.2	1	BC (2 × MIC)

[a] IC_{50} values were calculated from sigmoidal curves fitted to triplicate sets of dose–response data.

[b] MIC_{90} values are means of triplicates. Ratio, GASTD+Fe/GASTD. All values >l, <l, >0.5, and ≤0.5 were rounded to the nearest whole number, to 1, and to one significant digit, respectively.

[c] Mode of action was evaluated in GASTD in duplicate. The concentration at which each compound was tested for mode of action is indicated between parentheses.

[d] Some bactericidal activity detected, yet below the 99% killing criterion set for defining bactericidal mode of action. BS, bacteriostatic; BC, bactericidal; nd, not determined.

Bioorg Med Chem Lett. Author manuscript; available in PMC 2012 November 1.

Table 4

Antimicrobial activity against *Y. pestis*

Compound	IC_{50}[a] (μM)		Ratio	MIC_{90}[b] (μM)		Ratio	Mode of action[c]
	PMHD+Fe	PMHD		PMHD+Fe	PMHD		
DAP series							
1	>8	9	nd	>8	31	nd	BC (1 × MIC)
2	>31	20	>2	>31	>31	nd	nd
3	>31	>31	nd	>31	>31	nd	nd
4	>16	>16	nd	>16	>16	nd	nd
5	>250	>250	nd	>250	>250	nd	ml
6	>31	>31	nd	>31	>31	nd	nd
7	>31	8	>4	>3l	>31	nd	nd
8	>31	13	>2	>31	>31	nd	nd
9	>63	181	nd	>63	>250	nd	nd
10	>31	>62	nd	>31	>63	nd	nd
11	>63	7	>9	>63	42	>l	BC (1 × MIC)
12	>63	>125	nd	>63	>125	nd	nd
13	>16	4	>4	>16	16	>1	BC (2 × MIC)
14	>63	5	>13	>63	21	>3	BC (2 × MIC)
15	>16	>16	nd	>16	>16	nd	nd
16	>8	>8	nd	>8	>8	nd	nd
17	>63	>31	nd	>63	>31	nd	nd
18	>16	>31	nd	>16	>3l	nd	nd
19	>31	8	>4	>31	>31	nd	nd
20	>31	>16	nd	>31	>16	nd	nd
21	>16	>31	nd	>16	>31	nd	nd
22	>16	>31	nd	>16	>31	nd	nd
BHHC series							
23	>4	>16	nd	>4	>16	nd	nd
24	>250	>250	nd	>250	>250	nd	nd
25	>2	>4	nd	>2	>4	nd	nd

Compound	IC_{50}[a] (μM)		Ratio	MIC_{90}[b] (μM)		Ratio	Mode of action[c]
	PMHD+Fe	PMHD		PMHD+Fe	PMHD		
26	>500	>500	nd	>500	>500	nd	nd
27	>59	4	>15	>59	15	>4	BC (2 × MIC)
28	>233	137	>2	>233	388	nd	BC (1 × MIC)
29	156	61	>3	233	116	2	BC (2 × MIC)
30	305	70	4	>500	250	>2	BC (2 × MIC)
31	>500	>500	nd	>500	>500	nd	nd
32	>4	0.04	>100	>4	0.2	>20	BC (2 × MIC)
Streptomycin	1	1	1	2	1	2	BC (2 × MIC)

[a] IC_{50} values were calculated from sigmoidal curves fitted to triplicate sets of dose response data.

[b] MIC_{90} values are means of triplicates. Ratio, PMHD+Fe/PMHD. All values >1, <l, >0.5, and ≤0.5 were rounded to the nearest whole number, to 1 and to one significant digit, respectively.

[c] Mode of action was evaluated in PMHD in duplicate The concentration at which each compound was tested for mode of action is indicated between parentheses. nd, not determined; US, bacteriostatic; BC, bactericidal.